Int. J. Heat Mass Transfer. Vol. 27, No. 8, pp. 1291–1309, 1984
Printed in Great Britain

0017–9310/84 $3.00 + 0.00

PREDICTION OF THE CONCENTRATION PDF FOR EVAPORATING SPRAYS

ALAN R. KERSTEIN
Thermofluids Division, Sandia National Laboratories, Livermore, CA 94550, U.S.A.

(*Received* 20 *July* 1983 *and in revised form* 3 *November* 1983)

Abstract—A model of an evaporating spray is proposed in which each droplet deposits vapor along a linear trajectory through a quiescent host gas. Assuming a random spatial distribution of trajectories and a Gaussian radial concentration profile about each trajectory, relationships are derived between the probability density function (pdf) for concentration and parameters governing individual-droplet processes. These results provide an efficient method for computing the pdf numerically. Furthermore, several distinctive features are predicted, including the occurrence of a plateau in the pdf at the instant of transition from a monotonic to a unimodal functional form.

NOMENCLATURE

- a area of circle of radius r
- c radial profile of vapor concentration for a single trajectory
- D vapor diffusion coefficient
- f pdf of vapor concentration
- F cdf of vapor concentration
- g pdf of m
- h pdf of λ
- I Fourier transform of input function
- L $n\lambda$
- m vapor mass deposition per unit trajectory length
- n areal number density of trajectories
- N generalization of n to the case of nonparallel trajectories
- r radial distance from the trajectory
- R radius of curvature of trajectory
- s argument of z
- S scale factor in formula for $f(y)$
- t time; argument of characteristic function
- w pdf of trajectory orientations
- $\mathbf{x}$ arbitrary location
- y vapor concentration, treated as a random variable
- Y partial sum over trajectories of y
- z input function
- Z indefinite integral of z.

Greek symbols

- γ 0.5572157... (Euler's constant)
- κ cumulant of $f(y)$
- λ width parameter in the radial profile of vapor concentration
- τ inverse strain rate
- ϕ characteristic function of the concentration pdf
- Φ characteristic function of the pdf of Y
- ψ joint pdf of m and λ
- $\hat{\Omega}$ trajectory orientation vector.

1. INTRODUCTION

THE PROBABILITY density function (pdf) for species concentration is widely recognized to be a key quantity in the theoretical modeling and experimental characterization of mixing processes in fluids [1]. The physical systems usually considered are single-phase (liquid or gas), and fluid turbulence is the mixing mechanism responsible for random variation of the species concentration. In two-phase systems consisting of a dispersed phase in a continuum (sprays, particle-laden flows, etc.), there are additional sources of random variation. In sprays, the locations, sizes and compositions of individual droplets may vary randomly. Some consequences of the random spatial distribution of droplets have previously been analyzed for combusting sprays with the droplets at rest relative to the gas [2]. Here, the statistics of a collection of vaporizing droplets in motion relative to a quiescent gas phase are analyzed in order to predict the pdf for vapor concentration in terms of parameters governing individual-droplet processes.

The motivation for considering this problem arises primarily in combustion applications, although the results are more widely applicable. The motivation is twofold. First, the concentration pdf influences the mean rate of vaporization, often the crucial quantity determining the design of a combustor. The full pdf is required because the vaporization rate is a strongly non-linear function of vapor concentration, so estimates based on the mean vapor concentration may be inaccurate. Second, the concentration pdf can be used to determine what fraction of space contains a flammable mixture, information which has proven useful in other contexts in studies of ignition and flame propagation [3].

The problem of predicting the concentration pdf for a spray can be approached from a number of viewpoints. One possible approach is the logical extension of recent efforts to model the hydrodynamics and transport properties of assemblages of spheres in a flow [4, 5]. By coupling the gas-phase model to a model of individual-droplet internal circulation, transport and evaporation, a complete solution for the flowfield in a spray is envisaged. The concentration pdf or any other desired quantity can be computed from the complete solution. However, this approach is presently tractable only for periodic arrays of droplets and therefore cannot

incorporate the influence of the random spatial distribution of droplets. An alternative approach is to compute the hydrodynamics and transport for an individual droplet in a flow [6] for a variety of inlet conditions (vapor concentration, temperature, etc.) and then to average over the distribution of inlet conditions. However, the latter distribution, which includes the concentration pdf, is a function of individual-droplet processes, so it is not known *a priori*. The dependence of the concentration pdf on individual-droplet processes is the focus of the analysis presented herein. To this end, a model of the random geometry of an evaporating spray is proposed. The principal findings of this analysis are that the solution to the model provides a very efficient algorithm for computing the concentration pdf, and that some distinctive features of the concentration pdf can be inferred from general considerations.

The paper is organized as follows. A model of a vaporizing spray, denoted the 'basic model', is formulated. The model is solved to determine the concentration pdf, and properties of the solution are interpreted. To make the analysis concrete, a possible experimental realization of the basic model is described. The basic model does not incorporate sufficient information concerning the individual-droplet processes to provide an adequate representation of the interior of a spray. The model is therefore generalized, and resultant properties of the concentration pdf are investigated. Several distinctive features of the concentration pdf are predicted, and prospects for experimental confirmation of these features are assessed.

2. THE BASIC MODEL AND ITS GENERALIZATIONS

The total vapor concentration at any location in an evaporating spray is the sum of contributions from individual droplets. If the distribution functions governing the individual-droplet contributions are known, then the determination of the concentration pdf is a statistical problem solvable by standard methods, as demonstrated in Section 3.1. To characterize the individual-droplet contributions, we formulate a model, to be called the 'basic model', incorporating a set of assumptions concerning firstly, the trajectories of individual droplets through the host gas, and secondly, the spatial distribution of vapor relative to each trajectory. The basic model is the simplest case in which physically meaningful solutions to the statistical problem are obtained. Generalizations incorporating additional complexity are considered subsequently.

It is assumed that each droplet deposits vapor along a linear trajectory through the host gas, and that all trajectories are parallel. The trajectories are randomly distributed in space, that is, the points of intersection of the trajectories with a perpendicular plane are randomly distributed in that plane (planar Poisson process) with a mean number density, n, per unit area.

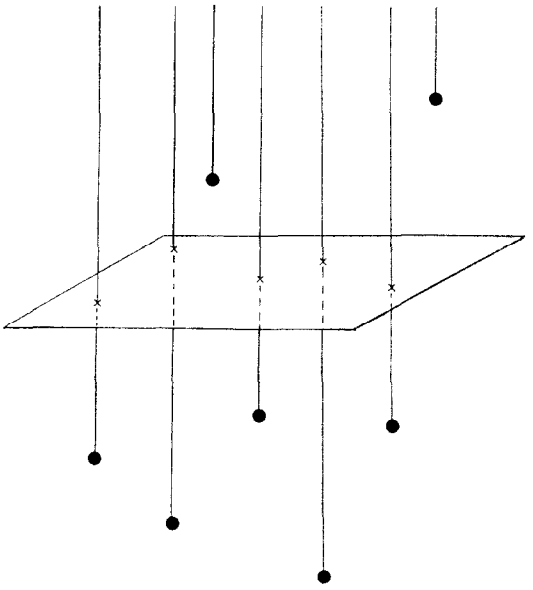

FIG. 1. Trajectories of droplets traversing the host gas. Dots are droplets, vertical rays are trajectories, and crosses are points of intersection of the trajectories with a perpendicular plane.

The geometry is shown in Fig. 1. As time passes, n increases as additional droplets cross the plane. (In Fig. 1, two droplets are shown which have not yet crossed the plane.) We will determine the concentration pdf at any location in the plane at a given instant, that is, for fixed n. In Section 4, the model is generalized to allow an arbitrary distribution of trajectory orientations. In all instances, however, droplet collisions are neglected.

Finally, assumptions are formulated concerning the distribution of vapor about each trajectory. The trajectory of a droplet may be regarded as the axis of a vapor trail deposited by that droplet. The spatial distribution of vapor is conveniently described in cylindrical coordinates with the axial coordinate along the trajectory. It is assumed that the vapor distribution is axisymmetric, and that the axial dependence of vapor concentration, c, is much weaker than the (radial) r-dependence, so that axial vapor transport can be neglected. The latter assumption is valid provided that the axial distance over which the droplet size, velocity or vaporization rate varies significantly is much greater than the droplet radius, r_d. Since the host gas is assumed to be quiescent, the only significant transport process far from the droplet is molecular diffusion in the radial direction, with the diffusivity, D, assumed constant. These assumptions are not precisely obeyed in evaporating sprays due to stirring of the gas by the moving droplets, and due to the temperature-dependence of the diffusivity. Nevertheless, they are appropriate modeling approximations in the present context. Under these assumptions, the radial profile of vapor concentration relaxes to the form

$$c(r) = \frac{m}{\lambda} \exp(-\pi r^2/\lambda), \tag{1}$$

where m is the mass of vapor deposited per unit trajectory length and $\lambda = 4\pi Dt$. (t is the time elapsed since passage of the droplet.) Equation (1) is valid in the limit $\sqrt{(Dt)} \gg r_d$. The rationale is as follows. Shortly after deposition of the vapor, the radial dependence of c is determined by the detailed dynamics of the evaporation process, and the width of the radial concentration profile is of the order of the droplet radius, r_d. For sufficiently large t, the width of the profile is of the order of the diffusion length, $\sqrt{(Dt)}$, and the shape of the profile becomes insensitive to details of the profile at early times. Specifically, the solution to the radial diffusion equation relaxes to the Gaussian distribution, reparameterized above for later convenience.

The Gaussian profile assumption is violated most severely in the immediate vicinity of a droplet. In this case, λ is very small so equation (1) predicts very large values of $c(0)$, values which may be unphysical since the vapor concentration cannot exceed the equilibrium vapor concentration at saturation. In Section 4.4, saturation effects are incorporated by means of a simple modification of the pdf, a modification which is valid provided that the mean vapor concentration is well below saturation.

For values of the diffusion length greatly exceeding the mean spacing between trajectories, the model is valid but not very interesting because the vapor is thoroughly mixed with the host gas and the spatial variation of concentration is insignificant. Therefore, to assure that the modeling assumptions are valid in a physically interesting regime, we require that $nr_d^2 \ll 1$, that is, the spray must be dilute. (This requirement is also a consequence of the neglect of droplet collisions, mentioned earlier.)

Returning to Fig. 1, the spatial distribution of concentration in the indicated plane is completely determined by the spatial distribution of trajectories and by the values of m and λ for each trajectory. The values of λ vary randomly due to the distribution of times elapsed since passage of the droplets through the plane. m also depends on the elapsed time because ambient conditions and therefore vaporization rates are time-varying. Thus, m is a random variable as well. (Distributions of droplet size, temperature or composition may also contribute to the random variation of m.)

In the basic model, m and λ are assumed to be constant for all trajectories, so the only source of randomness is the random spatial distribution of trajectories. This assumption is clearly unrealistic for prediction of the concentration pdf in the interior of the spray. However, there is an experimentally realizable configuration, described in Section 3.3, for which this assumption is appropriate. Furthermore, it is shown in Section 4 that the mathematical solution for the basic model is readily generalized to incorporate the random variation of m and λ. The pdf's for these random variables are inputs to the generalized solution for the concentration pdf. The mathematical results provide a very efficient method for computing the concentration pdf from the inputs, a method which may enhance prospects for an overall, self-consistent solution of the flowfield, as discussed earlier.

3. THE CONCENTRATION PDF FOR THE BASIC MODEL

3.1. *Derivation of the concentration pdf*

Based on the stated assumptions, the determination of the concentration pdf for the basic model is a well-posed mathematical problem. Given a set of points (the intersections of the trajectories with a perpendicular plane) randomly distributed with a mean number density, n, per unit area, and associated with each point a concentration profile, $c(r)$, given by equation (1), with m and λ constant, the problem is to determine the concentration pdf at any location in the plane. The mathematical problem as formulated can be solved rigorously by standard methods [7, 8]. Here, we present physically motivated derivations rather than rigorous proofs.

Henceforth, we refer to the points of intersection as centers, and denote their locations in the plane by the set of vectors $\{\mathbf{x}_j\}$. The total concentration at a given location $\mathbf{x}$, denoted $y(\mathbf{x})$, is given by

$$y(\mathbf{x}) = \sum_j y_j = \sum_j c(|\mathbf{x} - \mathbf{x}_j|), \tag{2}$$

where $y_j = c(|\mathbf{x} - \mathbf{x}_j|)$ is the contribution of the jth center and the summation is over all centers.

The concentration pdf, denoted $f(y)$, is a function of the three parameters n, m and λ. However, two of these parameters can be eliminated by choice of dimensional units, as shown later.

The derivation of the concentration pdf is based on the interpretation of probabilities as volume fractions. Namely, the probability that a measurement of y at an arbitrary location will fall within a given range $y' < y < y''$ is equal to the volume fraction for which y is in that range. To relate this interpretation to the geometry of Fig. 1, consider the plane to be a slab of infinitesimal thickness ε. Since the axial variation of y over a distance ε is negligible, the volume fraction in the slab for which y is within the given range is equal to ε times the area fraction of that volume projected onto a face of the slab. Rather than carrying the factor ε through the derivations, we reinterpret probabilities as area fractions.

Equation (1) can be transformed by the change of variables $a = \pi r^2$, giving

$$c(a) = \frac{m}{\lambda} \exp(-a/\lambda). \tag{3}$$

Since c is a decreasing function of a, this equation can be inverted to obtain

$$a(c) = \begin{cases} -\lambda \ln(\lambda c/m) & c < m/\lambda, \\ 0 & c \geqslant m/\lambda, \end{cases} \tag{4}$$

where $a(c)$ is the area in which the concentration exceeds c.

Initially, we assume that $c(a)$ is any decreasing function which is non-negative and finite for all $a > 0$ ($c(0)$ may be finite or infinite), and we derive $f(y)$ as a function of n and $c(a)$. Under these assumptions, the inverse function $a(c)$ exists and has the same interpretation as above. We begin by defining a new concentration profile

$$\tilde{c}(a) = \begin{cases} c(a) & a \leqslant a_0, \\ 0 & a > a_0, \end{cases} \tag{5}$$

where a_0 is a cutoff. (The limit $a_0 \to \infty$ will be taken later.)

To determine the pdf of y at an arbitrary location $\mathbf{x}$, we first assume that there is exactly one center within a distance r_0 of $\mathbf{x}$, where $\pi r_0^2 = a_0$, and we seek to determine the concentration pdf, $f_1(y_1)$, at $\mathbf{x}$. (The subscripts are a reminder that the concentration pdf in this case is different than the pdf for total concentration, y.) It follows immediately from equation (5) and the interpretation of probabilities as area fractions that

$$\begin{aligned} f_1(y_1)\,\mathrm{d}y_1 &= \text{Prob}\,[y_1 < c < y_1 + \mathrm{d}y_1] \\ &= \frac{1}{a_0}\,(a(y_1) - a(y_1 + \mathrm{d}y_1)) \\ &= \begin{cases} -\dfrac{1}{a_0}\dfrac{\mathrm{d}a}{\mathrm{d}y_1}\,\mathrm{d}y_1 & c(a_0) \leqslant y_1 \leqslant c(0), \\ 0 & \text{otherwise}, \end{cases} \end{aligned} \tag{6}$$

where $\mathrm{d}a/\mathrm{d}y_1$ means $\mathrm{d}a/\mathrm{d}c$ evaluated at $c = y_1$.

To proceed further, we need the characteristic function of $f_1(y_1)$

$$\phi_1(t) = \int_{-\infty}^{\infty} \mathrm{e}^{\mathrm{i}ty_1} f_1(y_1)\,\mathrm{d}y_1. \tag{7}$$

(The argument, t, of the characteristic function is different from the time variable introduced earlier. The notation is chosen for consistency with statistics literature.) The characteristic function is useful due to the following property [9]. If $y_1, \ldots, y_k$ are independent random variables with pdf's $f_1(y_1), \ldots, f_k(y_k)$, then the pdf of the random variable

$$Y_k = \sum_{j=1}^{k} y_j$$

has the characteristic function,

$$\Phi_k(t) = \phi_1(t)\phi_2(t)\cdots\phi_k(t),$$

where $\phi_j(t)$ is the characteristic function of $f_j(y_j)$. This property is essentially a restatement of the convolution theorem of Fourier analysis. It provides a straightforward method for obtaining the pdf of a sum of independent random variables whose pdf's are known.

Substitution of equation (6) into equation (7) gives

$$\phi_1(t) = -\frac{1}{a_0}\int_{c(a_0)}^{c(0)} \mathrm{e}^{\mathrm{i}ty_1}\frac{\mathrm{d}a}{\mathrm{d}y_1}\,\mathrm{d}y_1. \tag{8}$$

Since y_1 is now an integration variable, we can replace it by c (recalling the definition of $\mathrm{d}a/\mathrm{d}y_1$), giving

$$\begin{aligned} \phi_1(t) &= -\frac{1}{a_0}\int_{c(a_0)}^{c(0)} \mathrm{e}^{\mathrm{i}tc}\frac{\mathrm{d}a}{\mathrm{d}c}\,\mathrm{d}c \\ &= \frac{1}{a_0}\int_0^{a_0} \mathrm{e}^{\mathrm{i}tc(a)}\,\mathrm{d}a. \end{aligned} \tag{9}$$

We have obtained the characteristic function for the concentration pdf for one center within a distance r_0 of $\mathbf{x}$. If instead we have k such centers whose locations are statistically independent, then the analysis is the same for each center, so the concentration pdf associated with each center and the corresponding characteristic function are again given by equations (6) and (9), respectively. Using the property stated after equation (7), the characteristic function for the random variable, Y_k, representing the sum of contributions from the k centers is

$$\Phi_k(t) = \phi_1^k(t). \tag{10}$$

Since the locations $\mathbf{x}_j$ of the centers within a distance r_0 of $\mathbf{x}$ are realizations of a planar Poisson process, k is a random variable governed by the Poisson distribution with mean value na_0. Therefore [10]

$$\text{Prob}\,[k] = \frac{(na_0)^k\,\mathrm{e}^{-na_0}}{k!}. \tag{11}$$

The sum of contributions from these centers is the random variable y corresponding to the concentration profile, equation (5). Therefore

$$f(y) = \sum_{k=0}^{\infty} f_k(y|k)\,\text{Prob}\,[k], \tag{12}$$

where f_k is the pdf of total concentration conditioned on the realization of exactly k centers within a distance r_0 of $\mathbf{x}$. The pdf's in equation (12) may be expressed in terms of their characteristic functions by inverting the definition of the characteristic function (the inversion is unique [9]) to obtain

$$f(y) = \frac{1}{2\pi}\int_{-\infty}^{\infty} \mathrm{e}^{-\mathrm{i}ty}\,\phi(t)\,\mathrm{d}t, \tag{13a}$$

$$f_k(y|k) = \frac{1}{2\pi}\int_{-\infty}^{\infty} \mathrm{e}^{-\mathrm{i}ty}\,\Phi_k(t)\,\mathrm{d}t, \tag{13b}$$

where equation (13b) follows from the fact that f_k by definition is the pdf of the random variable Y_k. An expression for $\phi(t)$ is obtained by substituting equations (13a) and (13b) into equation (12), bringing the summation into the integrand on the RHS, and equating integrands. (The latter step is justified by the one-to-one correspondence of pdf's and characteristic functions.) The result is

$$\begin{aligned} \phi(t) &= \sum_{k=0}^{\infty} \Phi_k(t)\,\text{Prob}\,[k] \\ &= \exp\{na_0(\phi_1(t) - 1)\}. \end{aligned} \tag{14}$$

The second line is obtained by using equations (10) and (11) to evaluate the sum. This is a standard result, stated without proof in ref. [7].

$\phi(t)$ is expressed in terms of the radial concentration profile by substituting equation (9) into equation (14), giving

$$\phi(t) = \exp\left\{n \int_0^{a_0} (e^{itc(a)} - 1)\, da\right\}. \tag{15}$$

This is the characteristic function of y for the concentration profile $\tilde{c}(a)$. The cutoff is eliminated by taking the limit $a_0 \to \infty$. Formally, this simply involves substitution of ∞ for a_0 in equation (15). This is a non-trivial step, however, because it imposes the additional condition on $c(a)$ that it decreases rapidly enough as $a_0 \to \infty$ so that the integral remains finite in the limit. Suffice to say that this condition is always obeyed for concentration profiles encountered in the present physical application.

Thus, the characteristic function of y for the concentration profile $c(a)$ is

$$\begin{aligned}\phi(t) &= \exp\left\{n \int_0^{\infty} (e^{itc(a)} - 1)\, da\right\} \\ &= \exp\left\{-n \int_0^{c(0)} (e^{itc} - 1) \frac{da}{dc}\, dc\right\}. \end{aligned} \tag{16}$$

The change of integration variable in the last line is convenient for later applications.

The pdf of y is determined by substituting equation (16) into equation (13a), giving

$$f(y) = \frac{1}{2\pi} \int_{-\infty}^{\infty} dt\, e^{-ity} \times \exp\left\{-n \int_0^{c(0)} (e^{itc(a)} - 1) \frac{da}{dc}\, dc\right\}. \tag{17}$$

This result is valid for any radial profile $c(a)$, or equivalently, any inverse relation $a(c)$, obeying the conditions stated in the derivation. Equation (17) is essentially a standard result, since it is a corollary of equation (14). $f(y)$ can be computed using equation (17), and some of the numerical results below were originally obtained in this way. However, for the radial profile given by equation (3), it will be shown that a simpler representation of $f(y)$ is available. This alternative representation is a new result, valid only for the stated form of the radial profile, and has consequences which are not readily apparent from inspection of equation (17).

From equation (4), $da/dc = -\lambda/c$, so

$$\phi(t) = \exp\left\{n\lambda \int_0^{m/\lambda} \frac{dc}{c} (e^{itc} - 1)\right\}. \tag{18}$$

Defining $L = n\lambda$ and introducing the dimensionless variables $\hat{c} = \lambda c/m$ and $\hat{t} = mt/\lambda$, the pdf becomes

$$f(y) = \frac{1}{2\pi} \frac{L}{nm} \int_{-\infty}^{\infty} d\hat{t}\, e^{-i\hat{t}Ly/nm} \times \exp\left\{L \int_0^1 \frac{d\hat{c}}{\hat{c}} (e^{i\hat{t}\hat{c}} - 1)\right\}. \tag{19}$$

The product nm has dimensions of concentration. Since there are two dimensional quantities, concentration and length, we are free to choose units so that $n = m = 1$. Making this choice, and omitting the hat symbol from integration variables, we obtain

$$f(y) = \frac{L}{2\pi} \int_{-\infty}^{\infty} dt\, e^{-itLy} \exp\left\{L \int_0^1 \frac{dc}{c} (e^{itc} - 1)\right\}. \tag{20}$$

This expression depends only on the parameter L, which is the square of the ratio of the radial profile width to the mean spacing of trajectories. (In what follows, n and m are reintroduced only to clarify physical interpretations.)

We shall derive the following relation involving $f(y)$ and the cumulative distribution function (cdf), defined as $F(y) = \int_{-\infty}^{y} f(y')\, dy'$

$$\frac{y}{L} f(y) = F(y) - F\left(y - \frac{1}{L}\right). \tag{21}$$

First, we note that $f(y)$ must be zero for $y < 0$ since y cannot be negative. Therefore, the lower limit of integration in the definition of $F(y)$ is set to zero. Next, $f(y)$ is expressed as the sum of two quantities, $f(y) = f_+(y) + f_-(y)$, where $f_+(y)$ and $f_-(y)$ are obtained by breaking the dt-integral of equation (20) into two parts, extending over positive and negative t-values, respectively. Complex conjugation and the transformation $t \to -t$ in the expression for $f_+(y)$ gives the result $f_-(y) = f_+^*(y)$, so that

$$\begin{aligned} f(y) &= f_+(y) + f_+^*(y) \\ &= 2\,\mathrm{Re} f_+(y) \\ &= \frac{L}{\pi}\,\mathrm{Re} \int_0^{\infty} dt\, e^{-itLy} \exp\left\{L \int_0^1 \frac{dc}{c} (e^{itc} - 1)\right\} \\ &= \frac{L}{\pi}\,\mathrm{Re} \int_0^{\infty} dt\, e^{-itLy} \exp\left\{L \int_0^t \frac{dx}{x} (e^{ix} - 1)\right\}. \end{aligned} \tag{22}$$

The restriction of the dt-integration to positive t has facilitated the introduction of the new variable $x = ct$. This expression for $f(y)$ can be integrated to obtain the RHS of equation (21) in the form

$$\begin{aligned} F(y) - F\left(y - \frac{1}{L}\right) &= \frac{1}{\pi}\,\mathrm{Re}\, i \int_0^{\infty} dt\, e^{-itLy} \left(\frac{1 - e^{it}}{t}\right) \\ &\quad \times \exp\left\{L \int_0^t \frac{dx}{x} (e^{ix} - 1)\right\} \\ &= -\frac{1}{\pi L}\,\mathrm{Re}\, i \int_0^{\infty} dt\, e^{-itLy} \\ &\quad \times \frac{d}{dt} \exp\left\{L \int_0^t \frac{dx}{x} (e^{ix} - 1)\right\}. \end{aligned} \tag{23}$$

The latter form can be integrated by parts, giving

$$F(y)-F\left(y-\frac{1}{L}\right) = -\frac{1}{\pi L}\,\mathrm{Re}\,\mathrm{i}\,\mathrm{e}^{-\mathrm{i}tLy} \times \exp\left\{L\int_0^t \frac{\mathrm{d}x}{x}(\mathrm{e}^{\mathrm{i}x}-1)\right\}\Bigg|_{t=0}^{\infty} + \frac{y}{\pi}\,\mathrm{Re}\int_0^{\infty}\mathrm{d}t\,\mathrm{e}^{-\mathrm{i}tLy} \times \exp\left\{L\int_0^t \frac{\mathrm{d}x}{x}(\mathrm{e}^{\mathrm{i}x}-1)\right\}. \tag{24}$$

The second term on the RHS is equal to $(y/L)f(y)$. [Compare equation (22).]

The derivation of equation (21) is completed by showing that the first term on the RHS of equation (24) vanishes. At $t = 0$, this term is proportional to Re i, which is zero. As $t \to \infty$, this term is of order t^{-L} and therefore vanishes in the limit. To show this, we express the dx-integral in terms of the cosine integral, Ci(t), and the sine integral, Si(t), defined as [11]

$$\mathrm{Ci}(t) = \gamma + \ln t + \int_0^t \frac{\cos x - 1}{x}\,\mathrm{d}x, \tag{25}$$

$$\mathrm{Si}(t) = \int_0^t \frac{\sin x}{x}\,\mathrm{d}x, \tag{26}$$

where $\gamma = 0.5772157\ldots$ is Euler's constant. In terms of these functions, the dx-integral is equal to $\mathrm{Ci}(t) + \mathrm{i}\,\mathrm{Si}(t) - \gamma - \ln t$. The asymptotic properties of these functions are known [11]. As $t \to \infty$, $\mathrm{Ci}(t) \to 0$ and $\mathrm{Si}(t) \to \pi/2$, so in this limit we obtain a t-dependence of the form $\exp(-L \ln t) = t^{-L}$, which vanishes as $L \to \infty$. This completes the derivation of equation (21).

The key to the derivation was the transformation $x = ct$ which transferred the t-dependence of the innermost integral of equation (22) to an endpoint of integration. Such a transformation is possible only for the radial profile given by equation (3), suggesting that we are dealing with a system with some special properties. These special properties can be identified by numerical or analytical methods. Numerical results and their physical implications are presented first, followed by analytical interpretations.

3.2. *Results and interpretations*

Since $f(y) = (\mathrm{d}/\mathrm{d}y)F(y)$, equation (21) is a homogeneous, linear first-order differential equation for $F(y)$. The only unusual feature is its non-locality, namely the dependence of $f(y)$ upon $F(y-1/L)$. The requirements $F(y) = 0$ for $y < 0$ and $F(\infty) = 1$ uniquely determine the solution. The latter requirement, which is the normalization condition for the pdf, is not implicit in the differential equation because both the differential equation and the condition at $y < 0$ are homogeneous, so their solution contains an arbitrary scale factor. (Alternatively, the scale factor can be derived directly, as shown in the Appendix.)

Before examining the results, it is possible to anticipate certain features of the pdf from general considerations. In the limit $L \ll 1$, the vapor is essentially confined to the immediate vicinity of each trajectory, so the measured concentration at an arbitrary location is likely to be small. Therefore, the concentration pdf is expected to peak at a low value. Due to the small but non-vanishing probability that the selected location is very close to a trajectory, it is anticipated that the pdf will have a secondary peak and/or a tail that extends to high concentration values. In the limit $L \to \infty$, the system is fully mixed so the normalized concentration is equal to unity everywhere and $f(y) = \delta(y-1)$. For large but finite L, it is therefore expected that $f(y)$ will peak near $y = 1$ and will have a narrow spread about the peak (i.e. no long tails). These features are general and are applicable to single-phase turbulent mixing as well as sprays. However, the manner in which the system evolves from the small-L limit to the large-L limit is system-specific. The details of this evolution are illustrated by the L-dependence of the concentration pdf for the basic model, examined next, and more general models, examined in Section 4.

In Fig. 2, the pdf $f(y)$ as obtained by solving equation (21) [or equivalently, by evaluating equation (20)] is displayed for a sequence of L-values in the vicinity of $L = 1$. As anticipated, the pdf tends to peak at small y, in fact at $y = 0$, when L is small. The tendency at large L toward a distribution narrowly spread about $y = 1$ is already evident at $L = 2$. In other respects, however, the pdf exhibits features that are surprising in the context of past experience. The evolution of the pdf is marked by three distinctive features; cliffs occurring at $y = 1/L$ for $L < 1$, a plateau at $L = 1$, and a shift at $L = 1$ from monotonic distributions diverging at $y = 0$ to distributions peaking near $y = 1$. The interpretation of these features will be approached from several viewpoints, including a plausibility argument, two different mathematical derivations, and a physical interpretation including an assessment of prospects for experimental confirmation.

First, we consider why some sort of distinctive behavior might be expected at $y = 1/L$. Reintroducing the parameters n and m and recalling the definition of L, this value of y corresponds to a concentration equal to m/λ. According to equation (3), this is the largest concentration value which can be contributed by an individual trajectory, so in order to achieve a significantly greater y-value, two or more trajectories must be close enough so that they both contribute substantially to the concentration in some region. For small L, this is an unlikely event, so an abrupt drop-off of the concentration pdf beyond $y = 1/L$ might be anticipated. (In fact, distinctive features are predicted analytically at all integer multiples of $1/L$, but the effects at higher multiples are quantitatively insignificant.)

This argument suggests but does not prove the existence of a cliff, or more precisely a discontinuity in the derivative of $f(y)$, at $y = 1/L$. A mathematical derivation is conveniently obtained using equation

(21). Since the cdf is zero for negative y, $F(y-1/L)=0$ for $y<1/L$. Therefore, for $y<1/L$, equation (21) simplifies to

$$F(y)=\frac{y}{L}f(y)$$

$$=\frac{y}{L}\frac{\mathrm{d}F(y)}{\mathrm{d}y}, \tag{27}$$

whose solution is

$$F(y)=Sy^{L}, \tag{28}$$

or equivalently

$$f(y)=SLy^{L-1}, \tag{29}$$

where S is the scale factor mentioned earlier. Two of the three distinctive features of $f(y)$ follow immediately. Equation (29) confirms the existence of the plateau for $L=1$. It also confirms the shift in the form of the distribution at $L=1$. For $0<L<1$, $f(y)$ diverges at $y=0$, but for $L>1$, $f(0)=0$. (Monotonicity for $0<L<1$ is demonstrated by taking the y-derivative of equation (21), obtaining the result that $\mathrm{d}f(y)/\mathrm{d}y$ is negative for all $y>0$.)

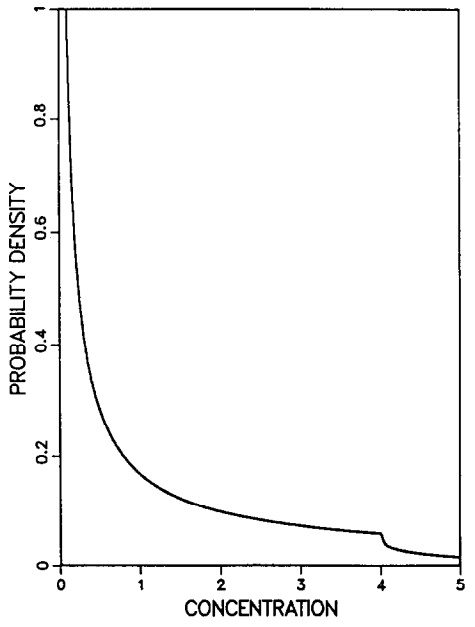

FIG. 2(a).

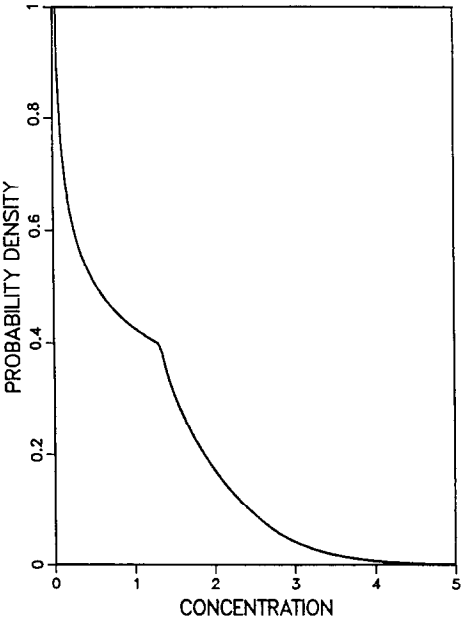

FIG. 2(c).

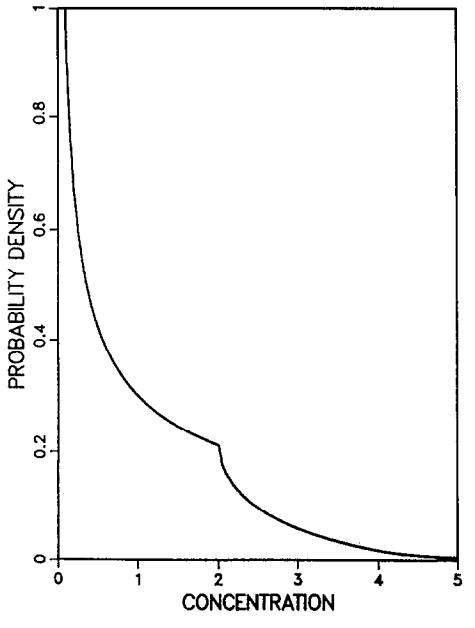

FIG. 2(b).

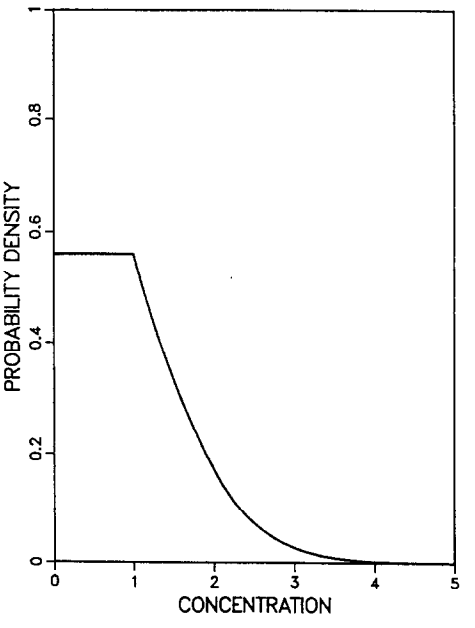

FIG. 2(d).

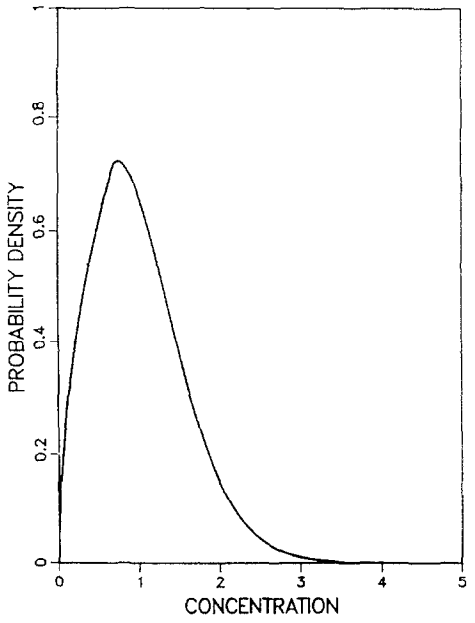

FIG. 2(e).

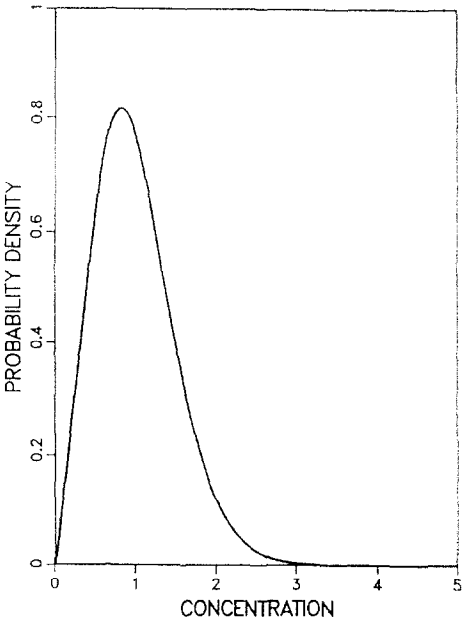

FIG. 2(f).

FIG. 2. Concentration pdf for the basic model (m and λ fixed). (a)–(f): $L = 0.25, 0.5, 0.75, 1.0, 1.5, 2.0$, respectively.

To confirm the cliff, we rewrite equation (21) in a form valid in the range $1/L < y < 2/L$ using equation (28)

$$\frac{y}{L} f(y) = F(y) - S\left(y - \frac{1}{L}\right)^L. \tag{30}$$

Taking the y-derivative of both sides and rearranging terms gives

$$\frac{df}{dy} = \frac{L-1}{y} f(y) - \frac{SL^2}{y}\left(y - \frac{1}{L}\right)^{L-1}. \tag{31}$$

For $0 < L < 1$, the last term on the RHS diverges as $y \to (1/L)_+$, while equation (29) indicates that the y-derivative of f is finite as $y \to (1/L)_-$. This confirms the cliff at $y = 1/L$ for $0 < L < 1$.

These results show that the distinctive features of the concentration pdf are intimately related to the representation for $f(y)$ given by equation (21). That representation is itself closely tied to the specific functional form, equation (3), assumed for $c(a)$. An alternative derivation of equation (28) is now outlined, a derivation which identifies the special property of the functional form, equation (3), which accounts for these results.

Recalling the representation of y in equation (2) as a sum of contributions y_j from individual centers, we relabel the individual contributions so that $y_1 > y_2 > y_3 > \ldots$ (y_j is now the jth 'order statistic' [12] of the individual contributions). Relabelled in this way, the individual contributions are no longer statistically independent since the placement of an individual contribution in the sequence depends upon the magnitudes of the other contributions.

We derive $F_1(y_1)$, which now is the cdf of the largest individual contribution. Since $a(c)$ is monotonic, $F_1(c) \equiv \text{Prob}[y_1 < c] = \text{Prob}[\text{no centers in } a(c)]$. The latter quantity is obtained by imbedding a in a large area A containing exactly nA centers, and by noting that the probability of no centers in a is $[(A-a)/A]^{nA}$. (Here it is useful to reintroduce dimensional parameters.) In the limit $A \to \infty$ we obtain the classical result [13]

$$\text{Prob}[\text{no centers in } a] = e^{-na}. \tag{32}$$

(In essence, we have rederived the Poisson distribution.) Using equation (4) for $a(c)$

$$F_1(c) = e^{-na(c)} = \begin{cases} (\lambda c/m)^{n\lambda} & c < m/\lambda, \\ 1 & c \geq m/\lambda, \end{cases} \tag{33}$$

or, setting $n = m = 1$ and replacing c by y_1

$$F_1(y_1) = \begin{cases} (Ly_1)^L & y_1 < 1/L, \\ 1 & y_1 \geq 1/L. \end{cases} \tag{34}$$

Thus, for $y_1 < 1/L$ the cdf of the largest individual contribution has the same functional form as the cdf for y, equation (28). This derivation is readily generalized to show that the cdf for the sum, Y_k, of the first k order statistics, for any positive integer k, is proportional to Y_k^L for $Y_k < 1/L$. This is a new result and is stronger than equation (28), which applies only to the infinite sum.

The special property of $c(a)$ which leads to equation (34) is that it has the same functional form as the Poisson distribution, equation (32). Consider the simplest case, $L = 1$, for which the distribution of y_1 is uniform over (0, 1). In this case, the probability that the center nearest to **x** [see equation (2)] falls within the

annulus $(a, a+da)$ corresponding to the concentration range $(c, c+dc)$ is independent of c. This is a unique property of the Poisson form of the concentration profile $c(a)$.

The Poisson form of the concentration profile is itself a consequence of the interpretation of probabilities as area fractions, which led to the change of variables $\pi r^2 = a$ in going from equation (1) to equation (3). This interpretation was motivated by the axisymmetric, approximately cylindrical geometry of the concentration profile with respect to the trajectory. In other words, the results which have been obtained are consequences of the fact that vapor transport in this system is locally two-dimensional.

In what follows, we consider first, the experimental realizability, and later, the generalizability of the results obtained thus far.

3.3. *Proposed experimental realization*

The basic model is not an adequate representation of the interior of a spray for reasons discussed in Section 2. However, there is an idealized configuration for which the assumptions of the basic model may be valid. The configuration is shown in Fig. 3.

Gas flows horizontally through a rectangular duct of uniform cross-section. A monodisperse spray of droplets moving vertically downward is continuously injected through a slit in the top face of the duct. The droplets deposit vapor as they transit the gas. They exit the flow (or are collected) at the bottom face. The droplet velocity greatly exceeds the gas velocity, and the droplets are large enough so that radial regression is slight during transit. The flux of droplets is low enough so that a droplet rarely is in the wake of another. Under these conditions, the droplets will deposit linear vapor streaks in the gas, as shown in the figure, with the mass, m, deposited per unit length roughly uniform along each trajectory and constant among droplets. (Relaxation of the latter assumption is considered in Section 4.4.)

The flow Reynolds number is chosen high enough so that the velocity profile is constant away from the wall boundary layer, but not so high as to induce instabilities. Therefore, the streaks will be convected downstream without significant distortion, except in the boundary layer. The parameter $L = n\lambda = 4\pi nDt$ is proportional to time and therefore, for constant velocity flow, is proportional to downstream distance from the slit.

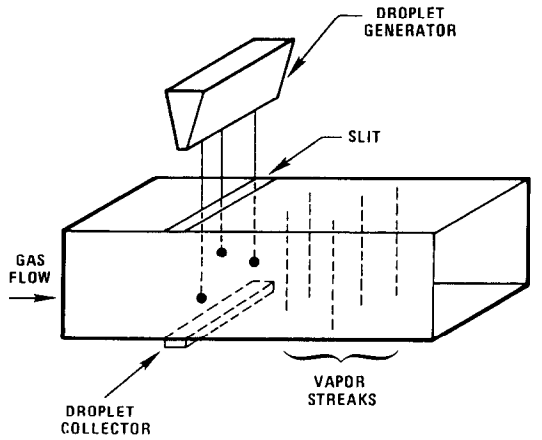

FIG. 3. Proposed experimental realization of the basic model.

Spatially-resolved concentration measurements at various downstream locations would thus provide the concentration pdf at various L values. Two of the empirical inputs, n and the flow velocity, are readily monitored. The parameter m is evaluated by monitoring the concentration at a far downstream location for which $L \gg 1$. There, the vapor is fully mixed and the vapor concentration is $c = nm$. Thus, all physical quantities are determined, and the measured pdf's can be directly compared to the predictions of Fig. 2 without introducing any additional empiricism.

As presented here, the configuration of Fig. 3 is an idealized thought experiment. Nevertheless, it serves several purposes. First, it shows that the analysis provides a complete and unambiguous prescription for comparing predictions to data. Second, it makes the analysis of the basic model more concrete by relating it to a physical configuration. Third and most important, it is shown in Section 4 that the features predicted thus far are of sufficient generality that they may be observable even in an imperfect realization of this configuration. Experimental validation of the analysis may therefore be feasible.

4. GENERALIZATIONS

4.1. *Distribution of trajectory orientations*

In the basic model, all droplet trajectories are parallel. The model is now generalized to allow any distribution of trajectory orientations. (Individual trajectories are still linear.) Since an additional element of randomness, the orientation distribution, is being introduced, a restatement of the statistical problem is required.

Each trajectory is associated with a vector oriented in the direction, $\hat{\Omega}$, of droplet motion. The orientation distribution may be characterized by a pdf $w(\hat{\Omega})$ defined over the unit sphere, where $w(\hat{\Omega})\,d\Omega$ is the probability that the orientation of a given trajectory is within an element $d\Omega$ of solid angle about $\hat{\Omega}$. For example, if the trajectories are all parallel with orientation $\hat{\Omega}_0$, then $w(\hat{\Omega}) = \delta(\hat{\Omega}-\hat{\Omega}_0)$. If the system is isotropic, then all orientations are equally likely and $w(\hat{\Omega}) = 1/4\pi$. If the trajectories are uniformly distributed within a cone angle θ_0, then $w(\hat{\Omega}) = 1/2\pi(1-\cos\theta_0)$ for $\theta < \theta_0$, zero otherwise. (For $\theta_0 = \pi$, this reduces to the isotropic distribution.) The result derived below is true for any distribution of trajectory orientations, in other words, for any pdf $w(\hat{\Omega})$ defined over the unit sphere.

In the present context, it is necessary to redefine the random spatial distribution of trajectories. The statistical assumption is as follows. Consider those trajectories whose orientations are within the solid

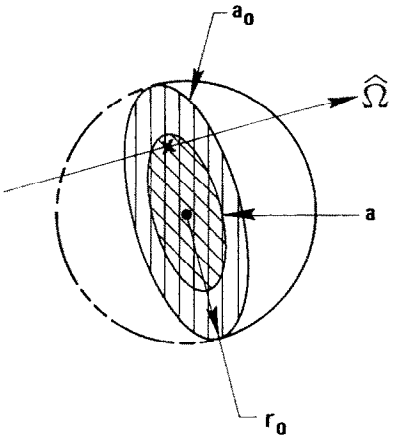

FIG. 4. Geometry for generalization to an arbitrary distribution of trajectory orientations.

angle $d\Omega$ about $\hat{\Omega}$. For any plane perpendicular to $\hat{\Omega}$, the locations of the points of intersection of these trajectories are assumed to be randomly distributed in the plane (planar Poisson process). This formulation is a natural generalization of the basic model, and it assures that the distribution of trajectories is spatially homogeneous.

As in Section 3.1, we seek the pdf of y at an arbitrary location $\mathbf{x}$. The first step is to consider a sphere of radius r_0 centered at $\mathbf{x}$, and to assume that exactly one trajectory, with orientation $\hat{\Omega}$, intersects the sphere. The geometry is shown in Fig. 4. The trajectory passes through the great circle (of area $a_0 = \pi r_0^2$) in the plane perpendicular to $\hat{\Omega}$. Using the definition of the random spatial distribution of trajectories, we can interpret probabilities as area fractions in the plane. In particular, the probability that the trajectory passes through a circle of area $a < a_0$ concentric with the great circle is a/a_0. By defining the radial (with respect to the trajectory axis) concentration profile $\tilde{c}(a)$ with cutoff a_0 as in equation (5), the pdf for concentration at $\mathbf{x}$ may be derived and the previous result, equation (6), is recovered. Since the orientation $\hat{\Omega}$ does not appear in the result, the concentration pdf $f_1(y_1)$ applies to any trajectory. Therefore, the characteristic function for Y_k, the sum of contributions from k trajectories, is again given by equation (10).

Now, however, the definition of k is different than before. k is now the random variable representing the number of trajectories intersecting a sphere of radius r_0. In order to proceed as before, it is necessary to show that k is governed by the Poisson distribution with mean value Na_0, where N is a constant which characterizes the system. Therefore, consider the number of intersections $k(\hat{\Omega})$ of the sphere by trajectories whose orientations are within the solid angle $d\Omega$ about $\hat{\Omega}$. This is equal to the number of intersections of the interior of the great circle whose plane is perpendicular to $\hat{\Omega}$. Since these intersections constitute a planar Poisson process, $k(\hat{\Omega})$ is governed by the Poisson distribution. The mean value of this distribution is proportional to a_0 and to $w(\hat{\Omega})\,d\Omega$, and therefore must be of the form

$$\langle k(\hat{\Omega})\rangle = Na_0 w(\hat{\Omega})\,d\Omega. \tag{35}$$

At this point, N has no obvious physical interpretation.

Regarding the element $d\Omega$ of solid angle as small but finite, k is a finite sum of the random variables $k(\hat{\Omega})$

$$k = \sum_{\hat{\Omega}} k(\hat{\Omega}). \tag{36}$$

We now employ the 'reproductive property' of the Poisson distribution [10], namely, a sum of independent, Poisson-distributed random variables is Poisson-distributed with mean equal to the sum of the mean values of those random variables. Therefore, k is Poisson-distributed with mean value

$$\begin{aligned}\langle k\rangle &= \sum_{\hat{\Omega}} \langle k(\hat{\Omega})\rangle \\ &= Na_0 \sum_{\hat{\Omega}} w(\hat{\Omega})\,d\Omega \\ &= Na_0.\end{aligned} \tag{37}$$

The last line of equation (37) is obtained by taking $d\Omega$ to be infinitesimal, converting the sum to an integral over the unit sphere, and applying the normalization condition for the orientation pdf.

The constant of proportionality, N, is now conveniently defined by setting $r_0 = 1$, which gives $a_0 = \pi$ and therefore $\langle k\rangle = N\pi$. The definition of N is then: $N = (1/\pi) \times$ (mean number of trajectories intersecting a sphere of unit radius). For the special case of parallel trajectories, $N = (1/\pi) \times (n\pi) = n$, for n as defined in the basic model. Thus, equation (11) is generalized to allow an arbitrary orientational distribution simply by replacing n by N. With this replacement, the remainder of the derivation of the concentration pdf proceeds as before.

These results also apply if m and λ are random variables. (The reasoning is essentially unchanged.) Bearing this in mind, the additional generalizations obtained below are derived for the special case of parallel trajectories.

4.2. *Mass and width distributions*

In the basic model, the values of the parameters m and λ are assumed to be the same for all trajectories. The inadequacy of this assumption for the interior of a spray is clear from consideration of Fig. 1. As noted earlier, λ is proportional to the time elapsed since passage of the droplet through the selected plane. Imagine that a constant flux of droplets passes through the plane starting at time t_0. Then at some later time t, the distribution of time elapsed since passage is the uniform distribution over the range $(0, t-t_0)$. If the flux of droplets varies with time, the distribution is modified accordingly. Thus, the distribution of λ depends upon time, spatial location (in the direction of droplet motion), and the complete time-history of droplet flux through the selected plane. Except for highly specialized configurations such as Fig. 3, the distribution of λ must be incorporated into the analysis.

The value of m varies from droplet to droplet because the instantaneous droplet vaporization rate depends upon the vapor concentration in the immediate vicinity of the droplet. The random spatial variation of the latter quantity is precisely the focus of this analysis, and a principal objective of this analysis is to determine the dependence of the pdf of vapor concentration on the distribution of m. However, the distribution of m at a given location is not uniquely determined by the concentration pdf at that location because the distribution of m is also affected by the distribution of λ and by random variation of droplet size, velocity, temperature and composition. The only way to close the mathematical system is to incorporate the relationships derived here into an overall model of the spray. In addition to their potential value as part of such an overall model, it is shown below that the relationships among the distributions of m, λ and vapor concentration lead to predictions of interest in their own right.

The most general description of the random variation of m and λ is obtained by defining the joint pdf of these parameters to be an arbitrary bivariate pdf $\psi(m, \lambda)$ in the domain of positive m and λ. Without loss of generality, this can be expressed as $\psi(m, \lambda) = g(m|\lambda)h(\lambda)$, where $g(m|\lambda)$ is the conditional distribution of m and $h(\lambda)$ is the marginal distribution of λ. This form is both mathematically convenient and readily interpreted physically.

The derivations of Section 3 can be generalized to incorporate arbitrary $\psi(m, \lambda)$, and the result will be given below. For clarity, the derivation is first presented for the special case in which m and λ are statistically independent random variables, so that $\psi(m, \lambda) = g(m)h(\lambda)$. It is then shown that only changes of notation are needed to obtain the more general result.

First, the distributions $g(m)$ and $h(\lambda)$ are discretized. Let $m_j = j\Delta m$ and $\lambda_k = k\Delta\lambda$ for positive integers j and k (which are unrelated to j and k as defined previously). Then the discretized distributions are sequences $\{g_j\}$ and $\{h_k\}$ such that

$$g_j \equiv \text{Prob}\,[m_{j-1} < m < m_j] = g(m_j)\Delta m,$$
$$h_k \equiv \text{Prob}\,[\lambda_{k-1} < \lambda < \lambda_k] = h(\lambda_k)\Delta\lambda. \tag{38}$$

(Later, the limits $\Delta m \to 0$ and $\Delta\lambda \to 0$ will be taken, converting certain sums to integrals.)

We seek a generalization of equation (18) for the characteristic function of the concentration pdf. Initially, only those trajectories for which $m = m_j$ and $\lambda = \lambda_k$ are to be included. These trajectories are randomly distributed in space with areal number density ng_jh_k (since they constitute a fraction g_jh_k of all trajectories). With the appropriate changes of notation, the assumptions in the derivation of equation (18) are satisfied, leading to

$$\phi_{jk}(t) = \exp\left\{ng_jh_k\lambda_k\int_0^{m_j/\lambda_k}\frac{dc}{c}(e^{itc}-1)\right\}$$
$$= \exp\left\{ng_jh_k\lambda_k\int_0^1\frac{d\hat{c}}{\hat{c}}(e^{im_jt\hat{c}/\lambda_k}-1)\right\}, \tag{39}$$

where the subscripts on ϕ denote the particular subset of trajectories which has been selected. In the second line, the dimensionless variable $\hat{c} = \lambda_k c/m_j$ has been introduced.

The random variable corresponding to ϕ_{jk} is denoted y_{jk}. The random variable y representing the totality of contributions from all trajectories is therefore $y = \sum_j\sum_k y_{jk}$. Using the property of characteristic functions stated after equation (7), the characteristic function of y is

$$\phi(t) = \prod_j\prod_k \phi_{jk}(t)$$
$$= \exp\left\{n\sum_j\sum_k g(m_j)\Delta m\, h(\lambda_k)\Delta\lambda\,\lambda_k \times\int_0^1\frac{d\hat{c}}{\hat{c}}(e^{im_jt\hat{c}/\lambda_k}-1)\right\}, \tag{40}$$

using the definitions of g_j and h_k. This expression is transformed as follows. First, the hat symbol is omitted. Second, the summations are brought inside the integral. Third, the limits $\Delta m \to 0$ and $\Delta\lambda \to 0$ are taken, converting the sums to integrals over the distributions $g(m)$ and $h(\lambda)$. Fourth, the angular bracket notation $\langle\ \rangle$ is introduced to represent the expectation of a random variable with respect to its distribution. Fifth, the dimensionless parameter $L = n\langle\lambda\rangle$ is introduced. The final result is

$$\phi(t) = \exp\left\{L\int_0^1\frac{dc}{c}(I(tc)-1)\right\}, \tag{41}$$

where

$$I(x) = \frac{1}{\langle\lambda\rangle}\int_0^\infty\int_0^\infty dm\, d\lambda\, g(m)h(\lambda)\lambda\, e^{imx/\lambda}. \tag{42}$$

Substituting equation (41) into equation (13a), the pdf of y is

$$f(y) = \frac{1}{2\pi}\int_{-\infty}^\infty dt\, e^{-ity}\exp\left\{L\int_0^1\frac{dc}{c}(I(tc)-1)\right\}. \tag{43}$$

In the special case $g(m) = \delta(m-\langle m\rangle)$, $h(\lambda) = \delta(\lambda-\langle\lambda\rangle)$, this reduces to equation (20) provided that units are chosen so that $n = \langle m\rangle = 1$. In what follows, these units are adopted except where explicit inclusion of n and $\langle m\rangle$ clarifies the physical interpretation.

Next, the generalization of equation (21) is derived. The reasoning which led to equation (22) is still applicable, giving

$$f(y) = \frac{1}{\pi}\text{Re}\int_0^\infty dt\, e^{-ity}\exp\left\{L\int_0^t\frac{dx}{x}(I(x)-1)\right\}, \tag{44}$$

where, as before, the change of variables $x = ct$ has removed the t-dependence from the inner integrand. This expression for $f(y)$ can be integrated to form the

quantity

$$F(y)-\int_{-\infty}^{\infty} ds\, z(s)F(y-s)$$
$$=\frac{1}{\pi}\,\mathrm{Re}\,i\int_0^{\infty} dt\, e^{-ity}\left(\frac{1-\int_{-\infty}^{\infty} ds\, z(s)\, e^{its}}{t}\right)$$
$$\times \exp\left\{L\int_0^t \frac{dx}{x}(I(x)-1)\right\}. \quad (45)$$

In this expression, $z(s)$ is an arbitrary function. However, if $z(s)$ is required to obey the relation

$$\int_{-\infty}^{\infty} ds\, z(s)\, e^{its} = I(t), \quad (46)$$

then equation (45) can be rewritten as

$$F(y)-\int_{-\infty}^{\infty} ds\, z(s)F(y-s)$$
$$= -\frac{1}{\pi L}\,\mathrm{Re}\,i\int_0^{\infty} dt\, e^{-ity}$$
$$\times \frac{d}{dt}\exp\left\{L\int_0^t \frac{dx}{x}(I(x)-1)\right\}. \quad (47)$$

As before, we integrate by parts, obtaining a term to be evaluated at $t = 0$ and ∞, and a term which, by comparison to equation (44), is found to be equal to $(y/L)f(y)$. The former term is shown in the Appendix to vanish unless $g(m)$ or $h(\lambda)$ has certain pathological (and patently unphysical) properties. Therefore, the generalization of equation (21) is

$$\frac{y}{L}f(y) = F(y)-\int_{-\infty}^{\infty} ds\, z(s)F(y-s), \quad (48)$$

where $z(s)$ satisfies equation (46).

To determine $z(s)$ in terms of $g(m)$ and $h(\lambda)$, equation (42) for $I(x)$ is substituted into equation (46). Expressing $z(s)$ as the inverse Fourier transform of $I(x)$

$$z(s) = \frac{1}{2\pi}\int_{-\infty}^{\infty} dx\, I(x)\, e^{-isx}$$
$$= \frac{1}{2\pi\langle\lambda\rangle}\int_0^{\infty} dm \int_0^{\infty} d\lambda\, g(m)h(\lambda)\lambda$$
$$\times \int_{-\infty}^{\infty} dx\, e^{-isx}\, e^{imx/\lambda}. \quad (49)$$

In the second line, the order of integration has been changed. Transforming the innermost integration variable to $\hat{x} = x/\lambda$, the innermost integral can be expressed as $2\pi\lambda\delta(m-s\lambda)$. Therefore

$$z(s) = \frac{1}{\langle\lambda\rangle}\int_0^{\infty} d\lambda\, \lambda^2 h(\lambda)\int_0^{\infty} dm\, g(m)\delta(m-s\lambda). \quad (50)$$

The dm-integral is equal to $g(s\lambda)$. Therefore

$$z(s) = \frac{1}{\langle\lambda\rangle}\int_0^{\infty} d\lambda\, \lambda^2 h(\lambda)g(s\lambda), \quad (51)$$

which is non-zero only for positive s.

Equations (48) and (51) establish the relationship between the distributions $g(m)$ and $h(\lambda)$ and the concentration pdf $f(y)$. The generalization to arbitrary $\psi(m,\lambda) = g(m|\lambda)h(\lambda)$ is straightforward. Since $g(m)$ always appears within the $d\lambda$-integral throughout the derivation, the entire derivation remains valid if $g(m)$ is replaced everywhere by $g(m|\lambda)$. Equation (48) is unchanged, but equation (51) becomes

$$z(s) = \frac{1}{\langle\lambda\rangle}\int_0^{\infty} d\lambda\, \lambda^2 h(\lambda)g(s\lambda|\lambda)$$
$$= \frac{1}{\langle\lambda\rangle}\int_0^{\infty} d\lambda\, \lambda^2\psi(s\lambda,\lambda). \quad (52)$$

Equations (48) and (52) constitute the most general representation of the concentration pdf obtained in this analysis, incorporating random trajectory locations (and random orientations, as in Section 4.1) and random variations of the parameters m and λ governing the radial concentration profile, including correlations between m and λ.

In what follows, equation (51) is employed, although the results generalize to equation (52) unless noted otherwise.

4.3. *Consequences and interpretations*

Within the framework of the modeling assumptions, the influence of individual-droplet processes on the concentration pdf $f(y)$ is expressed through the function $z(s)$, which we call the 'input function'. As in Section 3.2, equation (48) together with the non-negativity of y and the pdf normalization condition uniquely determine $f(y)$ for given $z(s)$. Before considering the converse question, some properties of $z(s)$ are noted.

It is easily shown that $z(s)$ has the mathematical properties of a pdf ; namely it is non-negative and its integral over $(-\infty, \infty)$ is unity. The product $s\lambda$ appears as the argument of the distribution g in equation (51). Therefore, it may be conjectured that s corresponds to the quantity m/λ, which in turn is equal to $c(0)$. [Compare equation (1).] However, the pdf of the latter quantity, obtainable by standard transformation-of-variables methods, is $\int_0^{\infty} d\lambda\, \lambda h(\lambda)g(s\lambda)$, which is different from equation (51). There does not appear to be an obvious physical interpretation of $z(s)$.

We now consider whether equation (48) uniquely determines $z(s)$ for given $f(y)$. We start with the y-derivative of equation (48)

$$\frac{1}{L}\frac{d}{dy}yf(y) = f(y)-\int_{-\infty}^{\infty} ds\, z(s)f(y-s). \quad (53)$$

Taking the Fourier transform of both sides, and using equations (7) and (46), we obtain

$$\frac{1}{L}\int_0^{\infty} dy\, e^{ity}\frac{d}{dy}yf(y) = \phi(t)-I(t)\phi(t), \quad (54)$$

where the last term is obtained by applying the convolution theorem, or by integrating directly. On the LHS, the lower limit of integration is set to zero since

$f(y)$ vanishes for negative y. Integration by parts gives an endpoint term to be evaluated at $y = 0$ and ∞, and an integral. The endpoint term is of order $yf(y)$. For $f(y)$ to be normalizable, it must go to zero faster than $1/y$ as $y \to \infty$, so the endpoint term vanishes in this limit. If we assume that $yf(y)$ also vanishes in the limit $y \to 0$ (a reasonable assumption, in view of the results of Section 3.2 and their generalizations below) we are left with

$$-\frac{it}{L}\int_0^\infty dy\, e^{ity} yf(y) = \phi(t)(1-I(t)). \tag{55}$$

Solving for $I(t)$

$$\begin{aligned} I(t) &= 1+\frac{it}{L\phi(t)}\int_0^\infty dy\, e^{ity}\, yf(y) \\ &= 1+\frac{t}{L\phi(t)}\frac{d}{dt}\int_0^\infty dy\, e^{ity} f(y) \\ &= 1+\frac{t}{L\phi(t)}\frac{d}{dt}\phi(t) \\ &= 1+\frac{t}{L}\frac{d}{dt}\ln\phi(t). \end{aligned} \tag{56}$$

Since $z(s)$ is the inverse Fourier transform of $I(t)$, equation (56) can be used to determine $z(s)$ from $f(y)$. For a number of reasons, this may not be the most practical method for estimating the input function from a measured concentration pdf; nevertheless, this result does show that $f(y)$ uniquely determines $z(s)$.

The above results establish a one-to-one correspondence between the concentration pdf and the input function. Since $z(s)$ does not determine $g(m|\lambda)$ and $h(\lambda)$ uniquely, additional information is needed to determine the latter distributions unambiguously from concentration measurements.

For example, consider the situation discussed at the beginning of Section 4.2, in which it is known that the flux of droplets begins at time t_0 and is constant thereafter. At some later time t, the distribution $h(\lambda)$ is the uniform distribution over $(0, \lambda_0)$, where $\lambda_0 = 4\pi D(t-t_0)$ (recalling the definition of λ in Section 2). If the random variables m and λ are assumed to be statistically independent, then equation (51) can be used to determine g as a function of z. Since the manipulations are routine, they are omitted. The result is

$$g(\lambda_0 s) = \frac{1}{2\lambda_0}\left(s\frac{dz(s)}{ds}+3z(s)\right). \tag{57}$$

However, if the assumption of statistical independence is not justified for the physical configuration of interest, equation (52) must be used. In this case, the assumptions stated above are not sufficient to determine $g(m|\lambda)$ uniquely in terms of $z(s)$.

Various assumptions are now adopted concerning the functions z, g and h, and the impact of each assumption on features of the concentration pdf is examined.

First, we assume that the distribution of m has a positive lower bound, m_-, and that the distribution of λ has a positive upper bound, λ_+. From equation (51), this gives $z(s) = 0$ for $s < m_-/\lambda_+$. Under these assumptions, consider equation (48) in the interval $0 < y < m_-/\lambda_+$. The lower bound of the ds-integral can be set to m_-/λ_+. Therefore, for y in this interval, the argument of F is negative over the domain of the integral, so the integral vanishes. Consequently, equation (48) reduces to equation (27). The implications are the same as in the previous analysis of equation (27). At $L = 1$, a plateau is predicted for $0 < y < m_-/\lambda_+$. For $0 < L < 1$, $f(y)$ diverges at $y = 0$, but for $L > 1$, $f(0) = 0$. Monotonicity for $0 < L < 1$ is demonstrated, as before, by taking the y-derivative of equation (48), obtaining the result that $df(y)/dy$ is negative for all $y > 0$. However, the previously-predicted cliff does not occur unless $z(s)$ is singular at $s = m_-/\lambda_+$.

The assumption that the distributions of m and λ are bounded from below and above, respectively, is realistic in many situations. Since λ is proportional to the time elapsed since passage of the droplet, its distribution at any instant is bounded from above because the spray is of finite duration. Very small values of m are anticipated only in two situations. If the host gas is nearly saturated, m can be very small for droplets over a significant size range. Alternatively, in portions of the spray in which some of the droplets are disappearing, droplets of arbitrarily small size may be present in significant numbers. Except for these two situations, the assumption of a lower bound on m is reasonable. Therefore, the features predicted above may occur in a variety of spray configurations.

The assumptions can be relaxed even further by introducing the following technical condition. Assume that $Z(y) \equiv \int_0^y z(s)\,ds = o(y)$, that is, $Z(y)$ approaches zero faster than y as $y \to 0$. Then it can be shown (derivation is omitted) that all the features predicted above, with the possible exception of the plateau at $L = 1$, still occur. The significance of this result is that the predicted features may occur even if m does not have a lower bound.

4.4. *Applications*

Some of the modeling assumptions cannot conveniently be generalized in a quantitative way, but possible generalizations can be assessed qualitatively. These include the assumptions of linear trajectories, no gas-phase convection, Gaussian radial concentration profiles and the statistical independence of individual-droplet vaporization rates and locations.

The assumption that trajectories are linear leads to axisymmetric concentration profiles for which the solution of the diffusion equation relaxes to the form given by equation (1). If instead the trajectories have some curvature with a representative radius of curvature R, then the dimensionless parameter characterizing the resultant distortion of the concentration profiles is $R^2/\langle\lambda\rangle = nR^2/L$. For L of order unity, which is the regime in which the predicted

features of $f(y)$ are most distinctive, the condition for low distortion is $nR^2 \gg 1$.

Gas-phase convection can likewise distort the concentration profile. The influence of convection can be characterized by the strain rate, which is the magnitude of a typical velocity gradient and has units of $(\text{time})^{-1}$. Defining τ to be the inverse strain rate, and using the definitions of L and λ, the condition for low distortion due to convection for L of order unity is $4\pi nD\tau \gg 1$.

Another effect which can distort the concentration profile is saturation. The most immediate consequence of saturation is that predicted concentration pdf's, such as those of Fig. 2, which extend to arbitrarily high concentration values, must become unphysical beyond the saturation vapor concentration. Physically, the volume fraction which is at or near saturation increases as vapor accumulates, so a peak will develop in the concentration pdf near the saturation vapor concentration. The simplest modification of the present analysis consistent with this physical picture is to cut off the predicted pdf at the saturation concentration, replacing the tail with a δ-function at the saturation concentration. The weight of the δ-function is set equal to the area under the tail. This is likely to provide an accurate representation of the concentration pdf provided that the area under the tail is much less than unity. Therefore, present analysis is applicable primarily to the stage of spray evolution for which the instantaneous mean vapor concentration is well below saturation.

Finally, several statistical assumptions are implicit in the analysis. The assumption that the trajectories are distributed according to a planar Poisson process characterized by the constant n, and analogous assumptions in Section 4.1, imply that the system must be spatially homogeneous. This assumption can be relaxed to require only local homogeneity, that is, significant spatial variations of the parameter n (or N in Section 4.1) are allowed only on a scale much larger than the trajectory spacing.

Another implicit statistical assumption is the statistical independence of individual-droplet vaporization rates and locations. On physical grounds, there must be some correlation between these quantities because, for instance, a droplet riding in the wake of a preceding droplet will experience a higher-than-average ambient vapor concentration (as well as hydrodynamic effects), tending to reduce its vaporization rate. What is not known, and is difficult to anticipate, is whether in the aggregate these correlations are sufficient to impact the predictive capability of the present analysis. The best remedy for this uncertainty would be a test of the predictions under the most favorable experimental conditions which can be achieved, namely the configuration described in Section 3.3.

We reconsider the proposed experiment in light of the results of Sections 4.1 and 4.2. In particular, assumptions concerning m and λ can now be generalized. In the experiment, the variation of λ at a given downstream location will be of the order of $\langle\lambda\rangle$ times the ratio of the slit width to the downstream distance at which $L = 1$ (provided that this downstream distance is much greater than the trajectory spacing, of order $n^{-1/2}$). This ratio can be kept small by design. However, the variation of m due to distributions of droplet size, velocity and ambient conditions experienced by each droplet is harder to control. Therefore, to predict features of the concentration pdf it is appropriate to assume that $h(\lambda) = \delta(\lambda - \langle\lambda\rangle)$ but to adopt a non-singular form for $g(m)$. As an illustrative

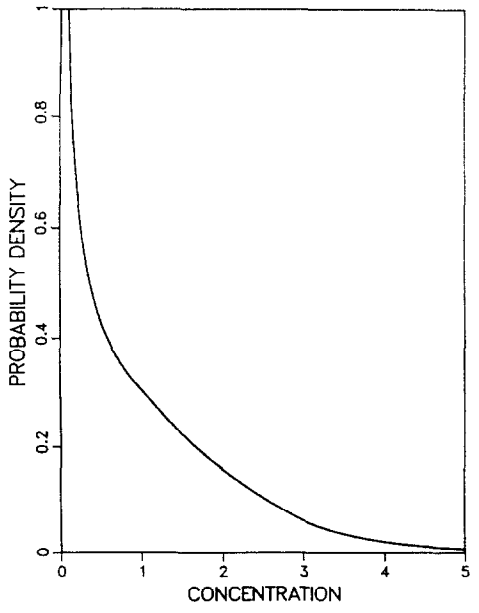

FIG. 5(a).

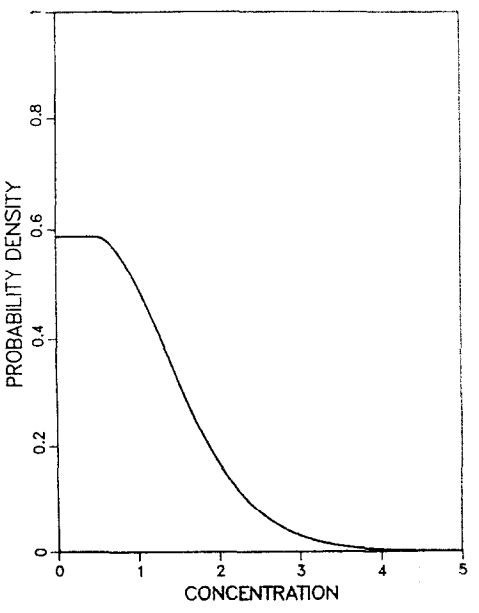

FIG. 5(b).

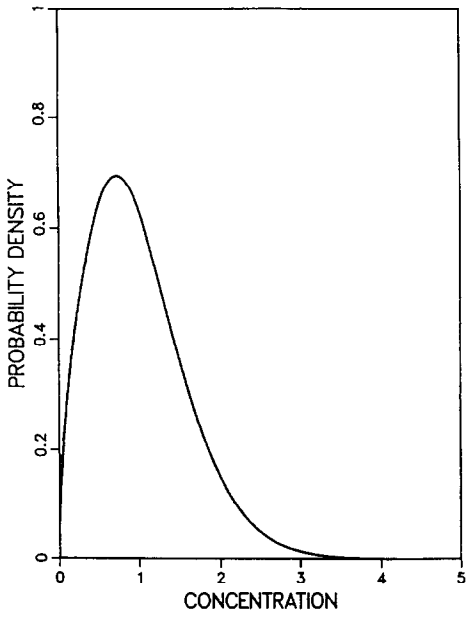

FIG. 5(c).

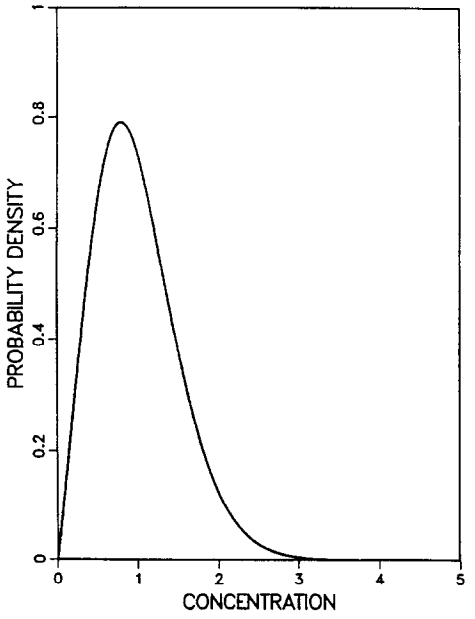

FIG. 5(d).

FIG. 5. Concentration pdf for a generalization of the basic model [m uniformly distributed over (0.5, 1.5), λ fixed]. (a)–(d): $L = 0.5, 1.0, 1.5, 2.0$, respectively.

case, we take $g(m)$ to be uniform over the domain $0.5 < m < 1.5$. Using equation (51), $z(s)$ is found to be the uniform distribution over the domain $(1/2L, 3/2L)$. Using this form for $z(s)$ in equation (48), the concentration pdf has been computed for several values of L, and the results are shown in Fig. 5. It is important to note that this is not an *a priori* prediction of the pdf, since it involves an assumed form for $g(m)$ which may require modification in order to fit the data. Nevertheless, these results do exhibit the plateau and the other distinctive features whose experimental confirmation would lend support to the statistical assumptions of the analysis. Furthermore, the measured pdf for any value of L is sufficient to determine $g(m)$ uniquely, since for $h(\lambda) = \delta(\lambda - \langle\lambda\rangle)$, we obtain $g(m) = (1/L)z(m/L)$. Verification that the same $g(m)$ fits the data for several different L values would therefore constitute a fully quantitative validation of the analysis.

For purposes of comparison, Fig. 6 displays the concentration pdf for the simplest assumptions applicable to the interior of a spray. If we adopt the assumption of uniform droplet flux [as in the derivation of equation (57)] and in addition assume that m is identical for all droplets, then we obtain

$$z(s) = \begin{cases} \dfrac{1}{2L^2 s^3} & s \geqslant 1/2L, \\ 0 & s < 1/2L. \end{cases} \tag{58}$$

In the absence of additional information, the results shown in Fig. 6 constitute a 'best guess' for the evolution of the concentration pdf for the interior of a spray. Measurements with sufficient resolution to identify departures from these results would motivate the introduction of more complicated forms of the input function.

Alternatively, these results for $f(y)$ can be used in a self-consistent computational solution for the evolution of the spray, as outlined in Section 1. In the most general case, the joint distribution $\psi(m, \lambda)$, defined in each computational cell, would be updated at each time-step based on the droplet vaporization and drag laws. As in deterministic spray simulations, the computational cells must be smaller than the distance over which droplet size or velocity varies significantly. The solution of equation (48) using equation (52) would provide an updated pdf. Since this procedure would be applied in every spatial cell at each time-step, the gain in efficiency due to use of equations (48) and (52) instead of, say, equations (42) and (44) could be crucial to the feasibility of the calculation. (Computational experience to date indicates a reduction of at least two orders of magnitude in computing time achieved by using the simpler equations.)

5. SUMMARY

A simple model of an evaporating spray has been proposed in which droplets deposit vapor along linear trajectories which are randomly distributed in space. It is assumed that the radial concentration profile about each trajectory relaxes to a Gaussian form expressed in terms of strength and width parameters m and λ which may vary randomly from trajectory to trajectory. Under these assumptions, relationships have been derived which determine the concentration pdf $f(y)$ in terms of the distributions of m and λ.

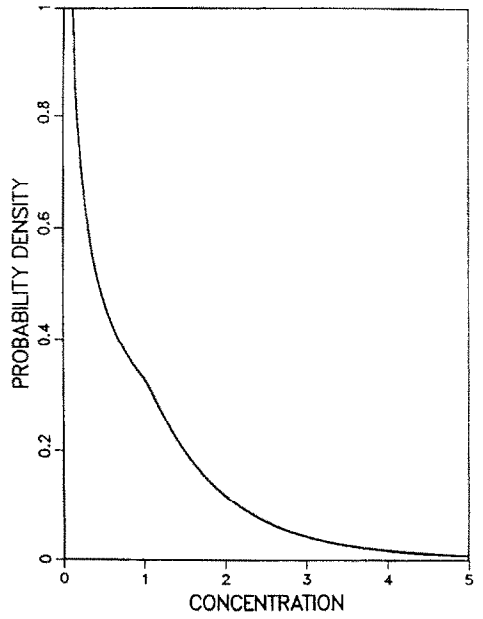

FIG. 6(a).

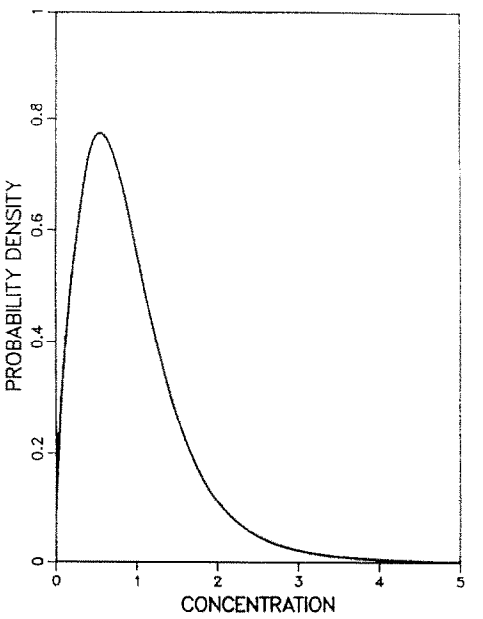

FIG. 6(c).

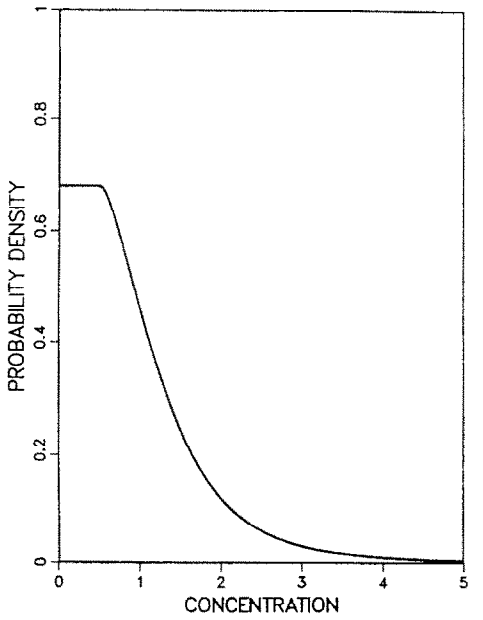

FIG. 6(b).

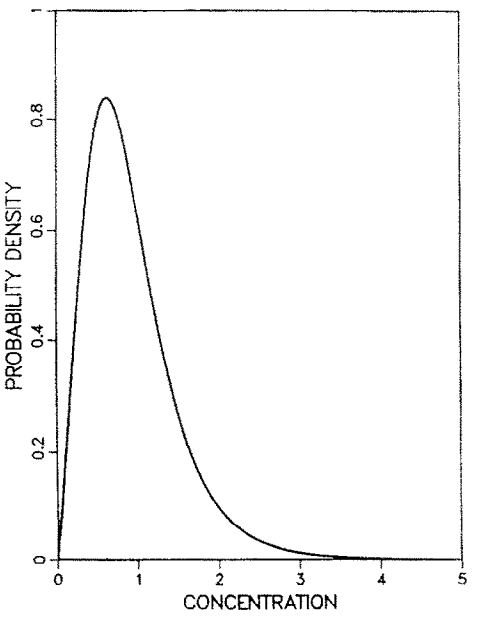

FIG. 6(d).

FIG. 6. Concentration pdf for the simplest model of the interior of a spray [m fixed, λ uniformly distributed over $(0, 1/2L)$]. (a)–(d): $L = 0.5, 1.0, 1.5, 2.0$, respectively.

The implications of these results are threefold. First, the results provide a very efficient method for numerical computation of the concentration pdf, which may enhance the capabilities of spray modeling codes. Second, an experimental configuration which would provide a quantitative test of the model has been identified. Third, distinctive features of the concentration pdf, including the occurrence of a plateau, are predicted under fairly general conditions, indicating that a qualitative test of the model may be feasible in complicated systems of practical interest. It has been shown that the distinctive features which are predicted are a direct consequence of the assumption that vapor transport in a non-convecting spray is locally two-dimensional.

Acknowledgements—The author would like to thank Jim Ringland for helpful discussions. This research was supported by the Office of Basic Energy Sciences, United States Department of Energy.

REFERENCES

1. R. W. Bilger, Turbulent flows with nonpremixed reactants, in *Turbulent Reacting Flows* (edited by P. A. Libby and F. A. Williams), Chap. 3. Springer, Berlin (1980).
2. A. R. Kerstein and C. K. Law, Percolation in combusting sprays I: Transition from cluster combustion to percolate combustion in non-premixed sprays, *Nineteenth Symposium (International) on Combustion*, Combustion Institute, Pittsburgh, Pennsylvania, pp. 961–969 (1983).
3. A. D. Birch, D. R. Brown and M. G. Dodson, Ignition probabilities in turbulent mixing flows, *Eighteenth Symposium (International) on Combustion*, Combustion Institute, Pittsburgh, Pennsylvania, pp. 1775–1780 (1981).
4. R. Tal and W. A. Sirignano, Cylindrical cell model for the hydrodynamics of particle assemblages at intermediate Reynolds numbers, *A.I.Ch.E. Jl* **28**, 233–237 (1982).
5. R. Tal, D. N. Lee and W. A. Sirignano, Hydrodynamics and heat transfer in sphere assemblages: Multisphere cylindrical cell models, AIAA-82-0302 (1982).
6. H. A. Dwyer, B. R. Sanders and F. Raiszadek, Ignition and flame propagation studies with adaptive numerical grids, *Combust. Flame* **52**, 11–23 (1983).
7. Y. S. Chow and H. Teicher, *Probability Theory*, Chap. 12. Springer, New York (1978).
8. D. L. Snyder, *Random Point Processes*, Chap. 7. Wiley, New York (1975).
9. S. S. Wilks, *Mathematical Statistics*, Chap. 5. Wiley, New York (1962).
10. S. S. Wilks, *Mathematical Statistics*, Chap. 6. Wiley, New York (1962).
11. M. Abramowitz and I. A. Stegun, *Handbook of Mathematical Functions*, Chap. 5. Dover, New York (1965).
12. S. S. Wilks, *Mathematical Statistics*, Chap. 8. Wiley, New York (1962).
13. S. Chandrasekhar, Stochastic problems in physics and astronomy, *Rev. Mod. Phys.* **15**, 1–89 (1943).
14. M. G. Kendall and A. Stuart, *The Advanced Theory of Statistics*, Vol. 1, Chap. 3. Griffin, London (1963).

APPENDIX

ADDITIONAL MATHEMATICAL RESULTS

Here, the scale factor defined in Section 3.2 is derived explicitly and the moments of $f(y)$ are determined in terms of the moments of $g(m)$ and $h(\lambda)$. In addition, the asymptotic normality of $f(y)$ is derived for the basic model.

A.1. *Derivation of the scale factor*

In Section 4.3, it was shown that $f(y) = SLy^{L-1}$ for $y < m_-/\lambda_+$, an expression which contains an as yet undetermined scale factor, S. This scale factor is now derived in terms of $g(m)$ and $h(\lambda)$. As before, generalization to the joint pdf $\psi(m, \lambda)$ is straightforward.

The derivation begins by substitution of $I(x)$, given by equation (42), into the innermost integral of equation (44) for $f(y)$. Changing the order of integration, the innermost integral of the expression for $f(y)$ becomes

$$\begin{aligned} L\int_0^t \frac{dx}{x}(I(x)-1) &= \int_0^\infty\int_0^\infty dm\, d\lambda\, g(m)h(\lambda)\lambda \int_0^t \frac{dx}{x}(e^{imx/\lambda}-1) \\ &= \int_0^\infty\int_0^\infty dm\, d\lambda\, g(m)h(\lambda)\lambda \\ &\quad \times\{\mathrm{Ci}(mt/\lambda)+i\,\mathrm{Si}(mt/\lambda)-\gamma-\ln(mt/\lambda)\} \\ &= -L\gamma - L\langle \ln m\rangle + \langle \lambda \ln \lambda\rangle - L\ln t \\ &\quad + \int_0^\infty\int_0^\infty dm\, d\lambda\, g(m)h(\lambda)\lambda \\ &\quad \times\{\mathrm{Ci}(mt/\lambda)+i\,\mathrm{Si}(mt/\lambda)\}, \end{aligned} \tag{A1}$$

where the dx-integral has been expressed in terms of the functions defined in equations (25) and (26). In the last line of equation (A1), the bracket notation introduced earlier denotes the expected value of the quantity in brackets with respect to the distributions $g(m)$ and $h(\lambda)$. Substitution of equation (A1) into equation (44) for $f(y)$, with the change of variables $u = yt$, gives

$$\begin{aligned} f(y) = y^{L-1}\frac{e^{-L\gamma}}{\pi} e^{-L\langle \ln m\rangle} e^{\langle \lambda \ln \lambda\rangle} \mathrm{Re}\int_0^\infty \frac{du}{u^L} e^{-iu} \\ \times \exp\left\{\int_0^\infty\int_0^\infty dm\, d\lambda\, g(m)h(\lambda)\lambda \right. \\ \left. \times\left[\mathrm{Ci}\left(\frac{mu}{\lambda y}\right)+i\,\mathrm{Si}\left(\frac{mu}{\lambda y}\right)\right]\right\}. \end{aligned} \tag{A2}$$

Since the y-dependence appearing outside the du-integral is precisely the y-dependence derived earlier for the domain $y < m_-/\lambda_+$, the du-integral must be independent of y in this domain. Therefore, we choose to evaluate the integral in the limit $y \to 0$, so that the previously stated asymptotic properties $\mathrm{Ci}(t) \to 0$ and $\mathrm{Si}(t) \to \pi/2$ as $t \to \infty$ can be employed.

Since it was shown in Section 4.3 that $f(y)$ is continuous at $y = 0$ for $L > 1$, it is valid for $L > 1$ to set y equal to zero in the du-integral and employ the asymptotic properties immediately. For $L \leqslant 1$, however, $f(y)$ is discontinuous at $y = 0$, so the asymptotic properties cannot be employed directly. However, the result obtained below, equation (A5), is an explicit analytic function of L, so its validity for $L \leqslant 1$ follows by analytic continuation from $L > 1$. This analytic continuation is permitted because $f(y)$ is analytic in L in a neighborhood of $y = 0$, as seen by inspection of equation (44).

Proceeding with substitution of the asymptotic values, we obtain

$$f(y) = y^{L-1}\frac{e^{-L\gamma}}{\pi} e^{-L\langle \ln m\rangle} e^{\langle \lambda \ln \lambda\rangle} \mathrm{Re}\, e^{iL\pi/2}\int_0^\infty \frac{du}{u^L} e^{-iu}. \tag{A3}$$

The integral is a combination of standard forms which can be evaluated explicitly, giving the result

$$\mathrm{Re}\, e^{iL\pi/2}\int_0^\infty \frac{du}{u^L} e^{-iu} = \frac{\pi}{\Gamma(L)}. \tag{A4}$$

Therefore

$$f(y) = \frac{e^{-L\gamma}}{\Gamma(L)} e^{-L\langle \ln m\rangle} e^{\langle \lambda \ln \lambda\rangle} y^{L-1}. \tag{A5}$$

Comparing this to equation (29), the factor multiplying y^{L-1} is equal to SL, thus determining the scale factor S.

This result has been verified numerically by checking that the value of S given by equation (A5) is the same as the value of S obtained by applying the normalization condition $F(\infty) = 1$ in the computations of $f(y)$.

The simplest application of equation (A5) is to the determination of $f(y)$ at the plateau which occurs at $L = 1$ for the basic model. The result is $f(y) = e^{-\gamma} = 0.561459\ldots$ [compare Fig. 2(d)].

Equation (A5) is physically meaningful only if $\langle \ln m\rangle$ and $\langle \lambda \ln \lambda\rangle$ are finite. These conditions are always obeyed if m_- and λ_+ are positive and finite. Distributions $g(m)$ and $h(\lambda)$ can be constructed for which these conditions are violated; however, these distributions are highly pathological and of no physical interest.

This derivation provides the mathematical tools needed to prove the assertion which follows equation (47). Specifically,

we wish to show that the quantity

$$E \equiv -\frac{1}{\pi L}\,\mathrm{Re}\,\mathrm{i}\,\mathrm{e}^{-\mathrm{i}ty}\exp\left\{L\int_0^t \frac{\mathrm{d}x}{x}(I(x)-1)\right\}, \quad \text{(A6)}$$

evaluated at $t = 0$ and ∞, is zero. At $t = 0$, this quantity is proportional to Re i and therefore vanishes. For the other endpoint, we first rewrite this expression in the notation of equation (A1), obtaining

$$E = -\frac{\mathrm{e}^{-L\gamma}}{\pi L}\,\mathrm{e}^{-L\langle \ln m\rangle}\,\mathrm{e}^{\langle \lambda \ln \lambda\rangle} \times \mathrm{Re}\,\frac{\mathrm{i}\,\mathrm{e}^{-\mathrm{i}ty}}{t^L}\exp\left\{\int_0^\infty\int_0^\infty \mathrm{d}m\,\mathrm{d}\lambda\, g(m)h(\lambda)\lambda \times [\mathrm{Ci}(mt/\lambda)+\mathrm{i}\,\mathrm{Si}(mt/\lambda)]\right\}. \quad \text{(A7)}$$

Using the asymptotic properties of Ci and Si, the argument of the exponential function converges to $\mathrm{i}\,\pi L/2$ as $t \to \infty$. Therefore, the t-dependence of equation (A7) in this limit is t^{-L}, which vanishes at $t = \infty$. As before, the result is valid provided that $\langle \ln m\rangle$ and $\langle \lambda \ln \lambda\rangle$ are finite.

A.2. *Moments of $f(y)$*

A recursion relation for the moments of $f(y)$ in terms of the moments of the pdf $z(s)$ is obtained from equation (48). After multiplying by y^{j-1} and integrating over y, elementary manipulations give the result

$$\frac{j}{L}\langle y^j\rangle = \sum_{k=0}^{j-1}\binom{j}{k}\langle s^{j-k}\rangle\langle y^k\rangle. \quad \text{(A8)}$$

In particular, $\langle y\rangle = 1$ (as required), and

$$\mathrm{var}[y] = \langle y^2\rangle - \langle y\rangle^2 = \frac{L}{2}(\langle s^2\rangle + 2\langle s\rangle) - 1. \quad \text{(A9)}$$

Using equation (51) or (52), moments of z are obtained in terms of moments of g and h

$$\langle s^j\rangle = \frac{1}{L}\langle m^j\rangle\langle \lambda^{1-j}\rangle. \quad \text{(A10)}$$

Substitution into equation (A9) gives

$$\mathrm{var}[y] = \frac{1}{2}\left\langle\frac{1}{\lambda}\right\rangle(1+\mathrm{var}[m]). \quad \text{(A11)}$$

Equation (A11) is a remarkably simple expression for the variance of the concentration. The term in parentheses exhibits the contribution due to the variability of m relative to the variability due to the random spatial distribution of trajectories.

A.3. *Asymptotic normality*

Equation (41) is readily transformed into the Lévy–Khintchine representation, demonstrating that the pdf $f(y)$ is infinitely divisible [7] for general $z(s)$. Therefore, it is of interest to investigate the class of stable distributions [7] obtained in the limit $L \to \infty$. For general $z(s)$, this is presently an open question. However, to illustrate how the results of this analysis can be used to address such questions in a simple and direct manner, a condition for the asymptotic normality of the pdf is derived.

We begin by determining the cumulants [9] of $f(y)$, defined as the coefficients $\{\kappa_j\}$ in the following power series expansion of $\ln \phi(t)$

$$\ln \phi(t) = \sum_{j=1}^{\infty}\frac{\kappa_j}{j!}(\mathrm{i}t)^j. \quad \text{(A12)}$$

The cumulants are conveniently evaluated by substituting equation (42) into equation (41) and expanding $I(tc)$ in a Taylor series about $t = 0$. The result is

$$\ln \phi(t) = \sum_{j=1}^{\infty}\frac{\langle m^j\rangle\langle \lambda^{1-j}\rangle}{j!\,j}(\mathrm{i}t)^j. \quad \text{(A13)}$$

Comparing equation (A13) to the definition (A12), the cumulants are found to be

$$\kappa_j = \frac{1}{j}\langle m^j\rangle\langle \lambda^{1-j}\rangle = \frac{L}{j}\langle s^j\rangle, \quad \text{(A14)}$$

where the last result is obtained using equation (A10).

A condition for asymptotic normality follows immediately because a distribution is normal if and only if $\kappa_j = 0$ for $j \geq 3$ [14]. Therefore, $f(y)$ is asymptotically normal for given $z(s)$ if and only if the third and higher moments of $z(s)$ vanish faster than $1/L$ as $L \to \infty$. This condition is obeyed, for example, by the basic model, but is violated by $z(s)$ as given in equation (58).

PREDICTION DE LA PDF EN CONCENTRATION POUR UN JET DE GOUTTELETTES QUI S'EVAPORENT

Résumé—On propose un modèle de jet de gouttelettes dans lequel chaque gouttelettes dépose de la vapeur le long d'une trajectoire linéaire à travers un gaz immobile. Supposant une distribution spatiale statistique de trajectoire et un profil radial de concentration Gaussien autour de chaque trajectoire, des formules sont obtenues entre la fonction de densité de probabilité (pdf) pour la concentration et les paramètres qui commandent les processus pour la gouttelette individuelle. Ces résultats donnent une méthode efficace pour calculer numériquement la pdf. Plusieurs éventualités distinctes sont prédites, incluant la présence d'un plateau dans la pdf à l'instant de transition d'une forme monotone à une forme fonctionnelle unimodale.

BERECHNUNG DER WAHRSCHEINLICHKEITSDICHTE-FUNKTION DER KONZENTRATION FÜR VERDAMPFENDE SPRÜHNEBEL

Zusammenfassung—Es wird ein Modell für einen verdampfenden Sprühnebel vorgeschlagen, bei dem jeder Tropfen Dampf entlang einer geradlinigen Bahn durch ein ruhendes Gas abgibt. Under der Annahme einer zufälligen räumlichen Verteilung der Bahnen und eines Gauß'schen Konzentrationsprofils radial um jede Bahn werden Beziehungen zwischen der Wahrscheinlichkeitsdichte-Funktion (pdf) für die Konzentration und den Parametern, die das Verhalten der einzelnen Tropfen bestimmen, hergeleitet. Die Ergebnisse ermöglichen es, die pdf numerisch zu berechnen. Ferner können einige spezifische Merkmale berechnet werden, einschließlich der Existenz eines Plateaus in der pdf, wenn von der monotonen auf eine unimodale Form der Funktion übergegangen wird.

РАСЧЕТ ФУНКЦИИ РАСПРЕДЕЛЕНИЯ КОНЦЕНТРАЦИИ В ИСПАРЯЮЩИХСЯ РАСПЫЛЕННЫХ СТРУЯХ

Аннотация—Предложена модель испаряющейся распыленной струи, в которой каждая капля образует пар вдоль линейной траектории, проходящей через неполвижный газ. В предположении случайного пространственного распределения траекторий и гауссового радиального профиля концентрации вокруг каждой траектории выведены соотношения между функцией распределения (ФР) концентрации и параметрами, определяющими процессы на каждой капле. Полученные результаты позволяют предложить эффективный метод численного расчета ФР. Кроме того, найдено несколько специфических характеристик, в том числе появление плато в ФР в момент перехода от монотонного к унимодальному функциональному виду.